Inorganic Chemistry

Article

pubs.acs.org/IC

Excited-State Relaxation of Ruthenium Polypyridyl Compounds Relevant to Dye-Sensitized Solar Cells

Ryan M. O'Donnell,[†] Patrik G. Johansson,[†] Maria Abrahamsson,[‡] and Gerald J. Meyer*[,†]

[†]Departments of Chemistry and Materials Science and Engineering, Johns Hopkins University, 3400 North Charles Street, Baltimore, Maryland 21218, United States

[‡]Department of Chemical and Biological Engineering, Chalmers University of Technology, 41296 Göteborg, Sweden

ABSTRACT: Remarkably little is known about metal-to-ligand charge transfer (MLCT) excited-state relaxation pathways for the ruthenium polypyridyl compounds commonly utilized in dye-sensitized solar cells. Herein, we report variable-temperature photoluminescence studies of compounds of the general type *cis*-$Ru(LL)_2(X)_2$, where LL is a bipyridyl ligand and X is CN^- or NCS^-, and contrast them with the well-known $Ru(bpy)_3^{2+}$ and $Os(bpy)_3^{2+}$, where bpy is 2,2′-bipyridine, to identify relaxation pathways. In fluid acetonitrile and propylene carbonate solutions, excited-state relaxation was found to obey a first-order kinetic model. An Arrhenius analysis revealed internal conversion to two different states, assigned to an upper MLCT excited state and a ligand field excited state. Relaxation through the upper MLCT excited state typically displayed pre-exponential factors of 10^7−10^8 s^{-1} with activation energies of 400−900 cm^{-1}, while relaxation rates through ligand field states occurred with 10^{14}−10^{15} s^{-1} and activation energies of 4000−5000 cm^{-1}. Nonradiative decay through LF states was sensitive to the ligand identity, but in a manner that was not fully consistent with the spectrochemical series. Excited-state relaxation of *cis*-$Ru(dcbH_2)_2(NCS)_2$, where $dcbH_2$ is 4,4′-$(CO_2H)_2$-2,2′-bipyridine, sometimes termed N3, anchored to mesoporous TiO_2 or ZrO_2 thin films immersed in CH_3CN occurred through the upper MLCT excited state with activational parameters in surprisingly good agreement with those abstracted from data measured in fluid solution. An important finding from these studies is that the population of dissociative ligand field excited states is unlikely to lead to unwanted photochemistry of dye-sensitized solar cells based on *cis*-$Ru(LL)_2(NCS)_2$-type compounds at room temperature.

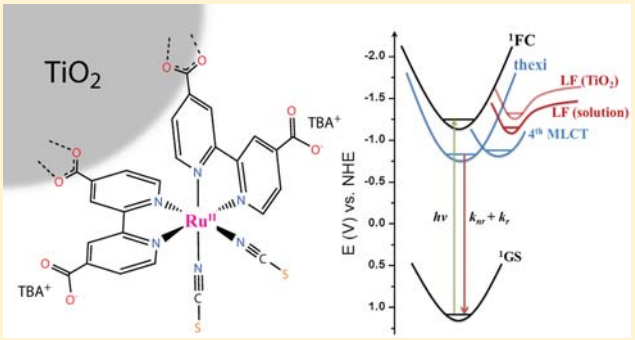

INTRODUCTION

Excited-state relaxation of the thermally equilibrated excited state of $Ru(bpy)_3^{2+}$ has been quantified in considerable detail by Crosby and co-workers.[1−3] Temperature-dependent photoluminescence (PL) measurements revealed the presence of three closely spaced metal-to-ligand charge transfer (MLCT) excited states that behave as a single state near room temperature. Later, experimental and theoretical analysis identified a fourth MLCT state that accounted for the weak temperature dependence near room temperature.[4−7] Excitation spectra revealed that intersystem crossing from upper excited states to the thermally equilibrated (thexi) states occurred with a quantum yield of unity.[3,8] Higher in energy are ligand field (LF) states, sometimes called d−d states, that are antibonding with respect to metal−ligand bonds, Scheme 1. Internal conversion from the MLCT states to the LF states can therefore lead to ligand loss photochemistry. As was emphasized by Crosby, the Ru center induces spin−orbit coupling that makes spin a poor quantum number for these electronic excited states.[3,9,10] Nevertheless, the initially formed excited state is necessarily singlet in character, while the thexi states have considerable triplet character. Herein, we use the term photoluminescence that implies no restrictions on the spin change that accompanies excited-state relaxation.

Scheme 1

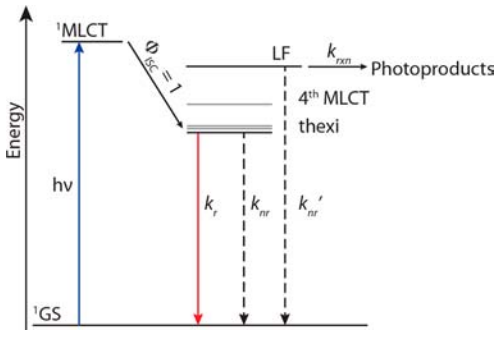

While it is often tacitly assumed that a Jablonski diagram like that shown in Scheme 1 for $Ru(bpy)_3^{2+}$ is applicable to all MLCT excited states, there is evidence to suggest otherwise.

Received: October 25, 2012
Published: January 15, 2013

   dx.doi.org/10.1021/ic302339a | *Inorg. Chem.* 2013, 52, 6839−6848

Scheme 2. Chemical Structures of Molecules Studied: (Left to Right) *cis*-Ru(bpy)$_2$(CN)$_2$, *cis*-Ru(bpy)$_2$(NCS)$_2$, and *cis*-Ru(dcbX$_2$)$_2$(NCS)$_2$, Where X = H (N3) or X = Tetrabutylammonium (N712)

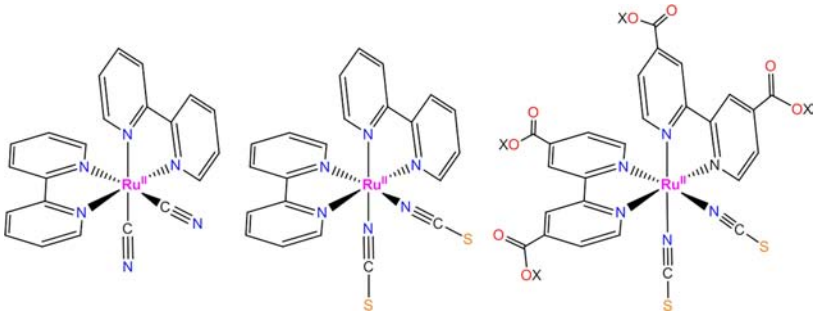

For example, nonunity intersystem crossing yields have been observed under a variety of conditions.[11−17] Excitation wavelength-dependent quantum yields for photochemical ligand loss have been reported.[18−21] Furthermore, the MLCT excited states are often found to be acutely sensitive to their external environment.[4,22−30] It is also noteworthy that excited-state relaxation pathways in compounds of lower symmetry, like the *cis*-Ru(bpy)$_2$X$_2$, where X is a halide or pseudohalide, have received remarkably little attention even though they represent the class of compounds most commonly utilized in dye-sensitized solar cells.[31−35] Here, we report photophysical studies of this type for compounds in fluid solution and anchored to semiconducting metal oxide surfaces.

Previous studies of MLCT excited states anchored to semiconductor surfaces have been limited, mainly because of rapid electron transfer to the semiconductor acceptor states.[36−43] However, it is possible to enhance the excited-state lifetime by shifting the semiconductor acceptor states to energies where electron transfer is unfavored.[44,45] For example, Sutin and Clark took advantage of the Nernstian shift of the rutile TiO_2 conduction band edge position to abstract reorganization energies for interfacial electron transfer; excited-state injection was favored under acidic conditions and was not observed when the pH was raised.[46] In another example, the MLCT excited states of *cis*-Ru(bpy)$_2$(ina)$_2^{2+}$, where ina is isonicotinic acid, anchored to mesoporous TiO_2 nanocrystalline (anatase) thin films displayed nonunity intersystem crossing yields with an increased activation barrier for MLCT → LF internal conversion.[47] Lateral intermolecular energy transfer across the surface has also been quantified in these same TiO_2 thin films.[48−51]

There exists compelling evidence that excited-state electron transfer from ruthenium polypyridyl compounds to anatase TiO_2 occurs on ultrafast time scales under many experimental conditions.[36−43] In addition to these subpicosecond electron transfer processes, there is evidence for slower interfacial electron transfer reactions that were likely occurring from the thexi state.[39−41,43] In principle, PL can report on the yields and rate constants for interfacial electron transfer from the thexi state. Several previous studies have reported data of exactly this type.[52−55] Furthermore, because PL is a contactless technique, it can, in principle, be used for the *in situ* characterization of operational dye-sensitized solar cells. As PL is an indirect probe of electron transfer, its use as an *in situ* tool for solar cell efficiency requires that the excited states be thoroughly characterized. Here, we report studies motivated toward this goal. Temperature-dependent PL studies of compounds of the general type *cis*-Ru(LL)$_2$(X)$_2$, where LL is a diimine ligand and X is CN^- or NCS^-, Scheme 2, have been contrasted with the well-known Ru(bpy)$_3^{2+}$ and Os(bpy)$_3^{2+}$, where bpy is 2,2′-bipyridine, to identify relaxation pathways. In addition, the photophysical properties of *cis*-Ru(dcbH$_2$)$_2$(NCS)$_2$, often called N3, anchored to mesoporous nanocrystalline (anatase) TiO_2 and ZrO_2 thin films have been characterized. An important finding from these studies is that the population of dissociative LF excited states is unlikely to lead to unwanted photochemistry in dye-sensitized solar cells based on these sensitizers. This conclusion stands in sharp contrast to what one would anticipate based on the spectrochemical series, and plausible explanations for this behavior are discussed.

EXPERIMENTAL SECTION

Materials. The following reagents were used as received from the following commercial suppliers: acetonitrile (Burdick & Jackson, spectrophotometric grade); ethanol (Pharmco-Aaper, 200 proof anhydrous); *tert*-butanol (Fisher, certified); propylene carbonate (Sigma-Aldrich, 99.7% anhydrous); deionized water; *n*-tetrabutylammonium hydroxide (TBAOH; Sigma-Aldrich, 1.0 M in methanol); potassium hydroxide (Fisher Scientific, >85%); potassium hexafluorophosphate (KPF_6; Aldrich, 98%); [Ru(bpy)$_3$]Cl$_2$·6H$_2$O (Aldrich, 99.95%); *cis*[Ru(dcbH$_2$)$_2$(NCS)$_2$] (Solaronix); titanium(IV) isopropoxide (Sigma-Aldrich, 97%); zirconium(IV) isopropoxide (Alfa Aesar, 70% in *n*-propanol); argon gas (Airgas, >99.998%); nitrogen gas (Airgas, 99.999%); and glass microscope slides (Fisher Scientific, 1 mm thick). [Ru(bpy)$_2$(CN)$_2$], [Ru(bpy)$_2$(NCS)$_2$], and [Os(bpy)$_3$](PF$_6$)$_2$ were available from previous studies.

Preparations. [Ru(bpy)$_3$](PF$_6$)$_2$ was prepared from the anion metathesis reaction of [Ru(bpy)$_3$]Cl$_2$·6H$_2$O with KPF_6. The neutral [Ru(dcbH$_2$)$_2$(NCS)$_2$] was fully deprotonated to form (TBA)$_4$[Ru(dcb)$_2$(NCS)$_2$] using TBAOH similar to the method reported by Nazeeruddin et al.[56]

Nanocrystallites of TiO_2 (anatase, ∼15 nm in diameter) and ZrO_2 (∼15 nm in diameter) were prepared by hydrolysis of Ti(*i*-OPr)$_4$ or Zr(*i*-OPr)$_4$, respectively, using a sol−gel method previously described in the literature.[57] The sols were cast as transparent mesoporous thin films by doctor blading onto glass microscope slides with the aid of transparent cellophane tape as a mask and spacer (∼10 μm thick). The films were sintered at 450 °C for 30 min under an atmosphere of O_2 flow and either used immediately for surface attachment or stored in an oven for future use. The thin films were treated with aqueous base (pH 11) for ∼15 min and rinsed with a 50:50 (v/v) mixture of CH_3CN/*tert*-butanol before sensitization in concentrated dyeing solutions. The sensitized thin films were then rinsed and stored in neat CH_3CN prior to use.

Spectroscopy. *UV−Visible Absorption.* Steady-state UV−visible (vis) absorption spectra were obtained on a Varian Cary 50 spectrophotometer at room temperature in 1.0 cm path length quartz or Pyrex cells.

Infrared Absorption. Attenuated total reflectance (ATR) FTIR absorbance spectra were obtained using a Thermo Scientific Nicolet Nexus 670 spectrophotometer with a Golden Gate ATR accessory.

dx.doi.org/10.1021/ic302339a | *Inorg. Chem.* 2013, 52, 6839−6848

The measurements were made under an N_2 atmosphere, and the spectra were averaged for 64 scans and background corrected with 4 cm^{-1} resolution.

^1H NMR. The ^1H NMR spectra were obtained on a Bruker Avance 400 MHz instrument in CH_3OD at room temperature (25.0 °C) and calibrated to residual solvent peaks.

Steady-State Photoluminescence. Steady-state photoluminescence (PL) spectra were obtained with a Spex Fluorolog spectrophotometer equipped with a 450 W Xe lamp or an argon ion laser for the excitation source. PL spectra of argon purged solutions were acquired at room temperature with photoluminescence detected at a right angle to the excitation beam. Quantum yields were measured versus $Os(bpy)_3^{2+}$ in CH_3CN as the standard ($\Phi_r = 0.005$) using the optically dilute method.[58,59] Sensitized metal oxide thin films were measured by placing the film diagonally in a 1.0 cm square quartz cell, exciting 45° to the surface, and monitoring from the front face of the sample.

Temperature-Dependent, Time-Resolved Photoluminescence. Nanosecond time-resolved PL data were acquired at a right angle to excitation with pulsed 450 or 500 nm laser light from a N_2 dye laser (Photon Technologies International, GL301, Coumarin 450 or 500 (Exciton)). Transient data were digitized on a computer-interfaced oscilloscope (LeCroy LT322) with 5 ns time resolution. Typically, 300 laser shots were averaged for each kinetic trace. For the temperature dependence studies, the sample temperature was maintained to ±0.1 °C using a liquid nitrogen cryostat (UniSoku CoolSpek USP-203-B).

Photolysis. Photolysis experiments were performed with the Spex Fluorolog spectrophotometer. Argon saturated samples were irradiated with light for 3 h at an elevated temperature of +70.0 °C, which was maintained to ±0.1 °C using a liquid nitrogen cryostat (UniSoku CoolSpek USP-203-B).

Data Fitting. Kinetic data fitting and Arrhenius analyses were performed in Origin 8.5 with least-squares error minimization accomplished using the Levenberg−Marquardt iteration method. Solution sample lifetimes were fit to single exponential decay kinetics over at least three half-lives, eq 1.

$$I(t) = I_0 \exp\left(\frac{-t}{\tau_{obs}}\right) + c \quad (1)$$

The temperature-dependent lifetimes were converted to observed rates and fitted to the modified Arrhenius expression, eq 2. Unless otherwise noted, the Arrhenius analyses were performed with only one activation energy term ($n = 1$) as the inclusion of a second ($n = 2$) did not improve the fit.

$$\frac{1}{\tau_{obs}} = k_0 + \sum_{i=1}^{n}\left[A_i \exp\left(\frac{-E_a}{k_B T}\right)\right] \quad (2)$$

RESULTS

Representative absorption and photoluminescence spectra of the *cis*-$Ru(bpy)_2(X)_2$ compounds dissolved in acetonitrile are shown in Figure 1. The fully deprotonated form of *cis*-$Ru(dcbH_2)_2(NCS)_2$, $(TBA)_4[Ru(dcb)_2(NCS)_2]$ also known as N712, was studied in most detail for solubility reasons. The three compounds possess two MLCT absorption bands centered around 500 nm and between 340 to 380 nm as well as ligand centered $\pi-\pi^*$ transitions between 290 and 310 nm. Visible light excitation resulted in room temperature photoluminescence (PL). The PL maximum of *cis*-$Ru(bpy)_2(NCS)_2$ at 745 nm was similar to that of $(TBA)_4[Ru(dcb)_2(NCS)_2]$, which occurred around 725 nm. The PL maximum of *cis*-$Ru(bpy)_2(CN)_2$ was blue-shifted in comparison to the isothiocyanate compounds and maximized at 680 nm; see Figure 1. The photophysical characteristics of the isothiocyanate and cyanide ligated compounds are given in Table 1 along with $Ru(bpy)_3^{2+}$ and $Os(bpy)_3^{2+}$ for comparison. All of the

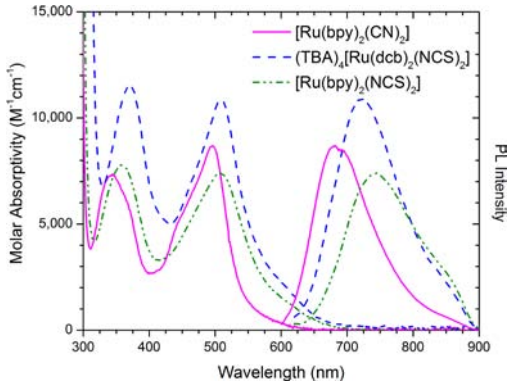

Figure 1. Absorption and photoluminescence spectra of *cis*-$Ru(bpy)_2(CN)_2$ (magenta), *cis*-$Ru(bpy)_2(NCS)_2$ (green), and $(TBA)_4[Ru(dcb)_2(NCS)_2]$ (blue) in acetonitrile.

compounds studied exhibited low energy absorption and PL maxima that were red-shifted as compared to $Ru(bpy)_3^{2+}$.

The isothiocyanate compounds were characterized via ATR-IR. A $\nu_{CN} = 2120\ cm^{-1}$ and $\nu_{CS} = 768\ cm^{-1}$ were observed in good agreement with literature values for N-coordinated isothiocyanate.[48,56] Likewise, the *cis*-$Ru(bpy)_2(NCS)_2$ sample used in this study exhibited $\nu_{CN} = 2099\ cm^{-1}$ and $\nu_{CS} = 795\ cm^{-1}$.[60,61] Had the S-coordinated isomer been present in an appreciable amount, lower energy stretches would have been expected with $\nu_{CN} \approx 2056\ cm^{-1}$ and $\nu_{CS} \approx 700\ cm^{-1}$.[62] There was no evidence for the presence of the *trans*-$Ru(dcbH_2)_2(NCS)_2$ isomer that exhibits a characteristic UV−vis absorption spectrum.[63] Furthermore, there is no literature precedence for formation of the *trans*-isomer by photoisomerization of *cis*-$Ru(dcbH_2)_2(NCS)_2$. The N-/N-coordinated *cis*-isomer is the only reported isomer for the $Ru(bpy)_2(NCS)_2$ compound.[63]

The ^1H NMR analysis of *cis*-$Ru(dcbH_2)_2(NCS)_2$ was in good agreement with previous studies. The ^1H NMR resonance at 9.58 ppm has been assigned to the N-/N-coordinated isothiocyanate isomer that integrated to ∼98−99% of the total concentration. Weak resonances at 9.92 and 9.51 ppm have been attributed to the S-coordinated isomers that comprised the remaining ∼1−2% of the sample.[62]

Pulsed light excitation of the compounds in acetonitrile yielded MLCT excited states that decayed to the ground state by a first-order kinetic model. The excited-state lifetimes obtained at room temperature, τ_o, for the isothiocyanate compounds were comparable to $Os(bpy)_3^{2+}$ ranging from 27 to 115 ns. The quantum yields for PL, Φ_{PL}, were quantified by the optically dilute method with $Os(bpy)_3^{2+*}$ employed as the actinometer.[58] A reported $\Phi_{PL} = 0.005$ for $Os(bpy)_3^{2+*}$ in argon-saturated acetonitrile was utilized, and any error in this value would result in systematic deviations of the data listed in Table 1.[59] The PL quantum yield for *cis*-$Ru(dcb)_2(NCS)_2^{4-}$ was 3.5×10^{-3} in acetonitrile and 2.0×10^{-3} in propylene carbonate, both values being slightly less than the reported value of 5×10^{-3} for $Os(bpy)_3^{2+}$ in acetonitrile and the measured value of 4×10^{-3} in propylene carbonate. The quantum yields for *cis*-$Ru(bpy)_2(NCS)_2$ and *cis*-$Ru(dcbH_2)_2(NCS)_2$ were quite small, on the order of $(5-7) \times 10^{-4}$. In addition to having a longer excited-state lifetime of around 240 ns in both solvents studied, *cis*-$Ru(bpy)_2(CN)_2$ also exhibited a PL quantum yield between that of $Ru(bpy)_3^{2+}$ and $Os(bpy)_3^{2+}$ equal to 1.6×10^{-2}.

dx.doi.org/10.1021/ic302339a | *Inorg. Chem.* 2013, 52, 6839−6848

Table 1. Photophysical Data of the Compounds in Solution at Room Temperature (+20 °C)

compound	solvent[a]	abs (nm)[b]	ε ($M^{-1}cm^{-1}$)[b]	PL (nm)	τ_o (ns)[c]	k_{obs} (s^{-1})	Φ_{PL}[d]	k_r (s^{-1})[e]	k_{nr} (s^{-1})[f]
$Ru(bpy)_3^{2+}$	ACN	450	14 600	615	825	1.2×10^6	0.062[†]	7.5×10^4	1.1×10^6
	PC	452		615	891	1.1×10^6	0.071[†]	8.0×10^4	1.0×10^6
$Os(bpy)_3^{2+}$	ACN	640	1800	736	59	1.7×10^7	0.005[‡]	8.5×10^4	1.7×10^7
	PC	640		736	52	1.9×10^7	0.004	7.7×10^4	1.9×10^7
$Ru(bpy)_2(CN)_2$	ACN	492	8700	682	244	4.1×10^6	0.016	6.6×10^4	4.0×10^6
	PC	495		679	239	4.2×10^6	0.016	6.7×10^4	4.1×10^6
$Ru(bpy)_2(NCS)_2$	ACN	505	7400	745	27	3.7×10^7	0.0006	2.2×10^4	3.7×10^7
	PC	507		743	29	3.4×10^7	0.0007	2.4×10^4	3.4×10^7
$Ru(dcb)_2(NCS)_2^{4-}$	ACN	507	10 900	723	115	8.7×10^6	0.0035	3.1×10^4	8.7×10^6
	PC	515		732	85	1.2×10^7	0.0020	2.4×10^4	1.2×10^7
$Ru(dcbH_2)_2(NCS)_2$	PC	529		780	30	3.3×10^7	0.0006	2.0×10^4	3.3×10^7

[a]ACN = acetonitrile; PC = propylene carbonate. [b]Maxima of the lowest energy MLCT absorption. [c]Lifetimes are ±5%. [d]PL quantum yields measured using $Os(bpy)_3^{2+}$ in ACN as standard with errors of ±10%. [e]$k_r = \Phi_{PL} \cdot k_{obs}$. [f]$k_{nr} = k_{obs} - k_r$. [†]*J. Am. Chem. Soc.* **1983**, *105*, 5583. [‡]*J. Phys. Chem.* **1986**, *90*, 3722. All measurements were obtained at +19 °C ± 2 °C. Wavelengths are ±2 nm.

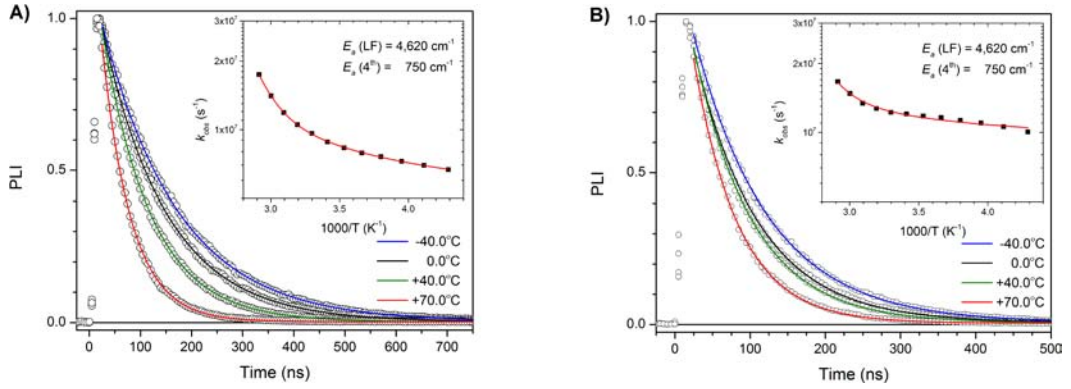

Figure 2. Time-resolved PL data measured after pulsed laser excitation of $(TBA)_4[Ru(dcb)_2(NCS)_2]$ in neat acetonitrile (A) and propylene carbonate (B) at the indicated temperatures. The insets depict Arrhenius analyses of the kinetic data.

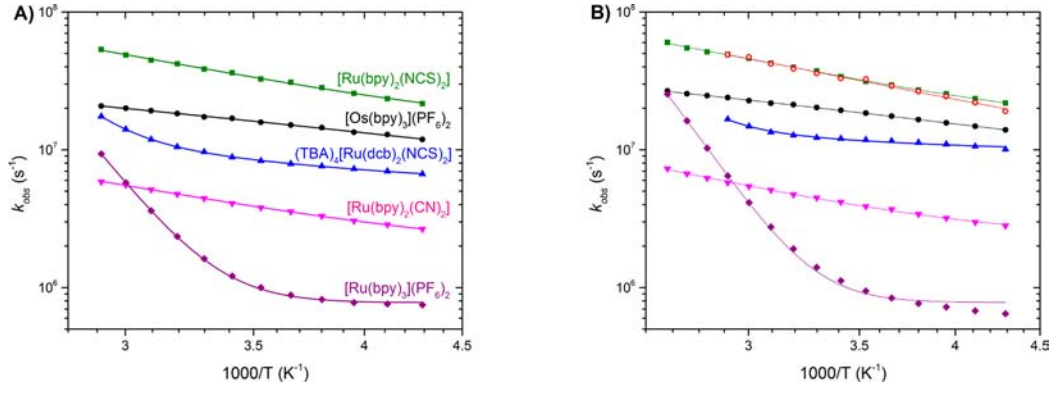

Figure 3. Arrhenius comparisons in acetonitrile (A) and propylene carbonate (B) of the studied compounds: $Ru(bpy)_3^{2+}$ (purple ◆); *cis*-$Ru(bpy)_2(CN)_2$ (magenta ▼); *cis*-$Ru(dcb)_2(NCS)_2^{4-}$ (blue ▲); $Os(bpy)_3^{2+}$ (black ●); *cis*-$Ru(bpy)_2(NCS)_2$ (green ■); and *cis*-$Ru(dcbH_2)_2(NCS)_2$ (red ○).

Manipulation of the sample temperature from −40.0 to +70.0 °C in acetonitrile and from −40.0 to +100.0 °C in propylene carbonate led to shorter observed excited-state lifetimes as expected for thermal activation to upper excited states. The observed relaxation rate constants for $Ru(bpy)_3^{2+}$*, $Os(bpy)_3^{2+}$*, *cis*-$Ru(bpy)_2(CN)_2$*, and *cis*-$Ru(bpy)_2(NCS)_2$* with respect to temperature could all be modeled with one activation parameter through an Arrhenius analysis. Two activation parameters were required to fit the Arrhenius data for $(TBA)_4[Ru(dcb)_2(NCS)_2]$, shown in Figure 2A, which yielded activation energies of 4620 and 750 cm^{-1} with corresponding pre-exponential factors of 1.7×10^{15} and 1.3×10^8 s^{-1}, respectively. Similar results were obtained in propylene carbonate solution, although the activation energy values needed to be fixed for the function to converge. Specifying activation energies of 4620 and 750 cm^{-1}, taken from the acetonitrile values, allowed the function to converge. The inset of Figure 2B depicts the fitted data with pre-exponential factors of 4.8×10^{15} and 9.7×10^7 s^{-1} that were in good agreement with the acetonitrile data. The temperature range for $(TBA)_4[Ru(dcb)_2(NCS)_2]$ in propylene carbonate

dx.doi.org/10.1021/ic302339a | *Inorg. Chem.* 2013, 52, 6839−6848

Table 2. Arrhenius Parameters for the Compounds in Fluid Solution

compound	solvent[a]	temp range (K)	k_0' (s^{-1})	k_1 (s^{-1})	k_1/k_0'	E_a (cm^{-1})
$Ru(bpy)_3^{2+}$	ACN	233−343	7.8×10^5	4.4×10^{14}	5.6×10^8	4240
	PC	233−373	7.8×10^5	4.0×10^{14}	5.1×10^8	4310
$Os(bpy)_3^{2+}$	ACN	233−343	5.1×10^6	8.9×10^7	17	410
	PC	233−373	6.6×10^6	1.0×10^8	16	430
$Ru(bpy)_2(CN)_2$	ACN	233−343	1.8×10^6	1.2×10^8	67	810
	PC	233−373	2.3×10^6	1.7×10^8	79	930
$Ru(bpy)_2(NCS)_2$	ACN	233−343	1.4×10^7	1.2×10^9	86	810
	PC	233−373	1.5×10^7	9.1×10^8	67	780
$Ru(dcb)_2(NCS)_2^{4-}$	ACN	233−343	5.5×10^6	1.7×10^{15}	3.1×10^8	4620
				1.3×10^8	24	750
	PC	233−343	9.7×10^6	8.3×10^{14}	8.6×10^7	4620[b]
				8.5×10^7	9	750[b]
$Ru(dcbH_2)_2(NCS)_2$	PC	233−313	9.5×10^6	6.6×10^8	70	670

[a]ACN = acetonitrile; PC = propylene carbonate. [b]Denotes values held constant during fitting; see text for details.

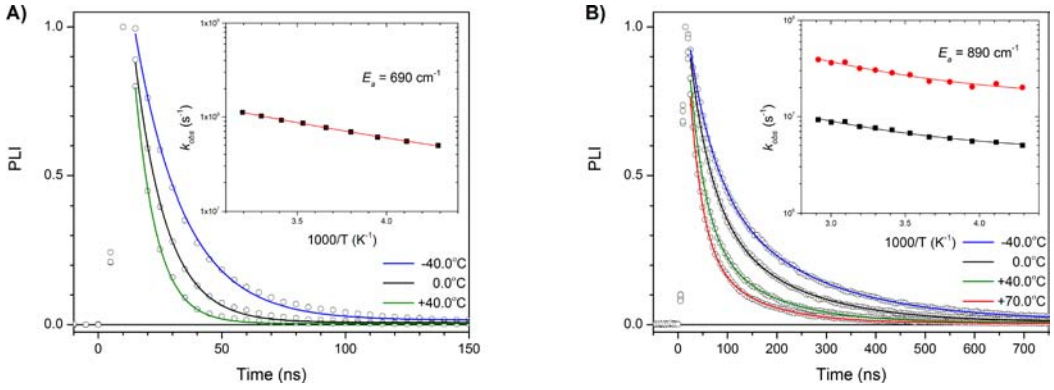

Figure 4. Time-resolved photoluminescence decays of $Ru(dcb)_2(NCS)_2/TiO_2$ (A) and $Ru(dcb)_2(NCS)_2/ZrO_2$ (B) in neat acetonitrile baths. Insets show the Arrhenius analyses with activation energies equal to 690 cm^{-1} for the TiO_2 data and 890 cm^{-1} for the ZrO_2 data.

Table 3. Arrhenius Parameters for *cis*-$Ru(dcb)_2(NCS)_2/MO_2$

MO_2	abs (nm)	PL (nm)	temp range (K)	k_0' (s^{-1})	k_1 (s^{-1})	k_1/k_0'	E_a (cm^{-1})
TiO_2	532	765	233−313	1.7×10^7	2.2×10^9	130	690
ZrO_2	508	725	233−343	4.2×1.0^6	2.2×10^8	52	890
				1.5×10^7	1.0×10^9	67	

was restricted from −40.0 to +70.0 °C as irreversible photochemistry was observed at higher temperatures.

The temperature-dependent relaxation rates are shown in Figure 3, and the excited-state decay parameters obtained from the Arrhenius analyses are collected in Table 2. The $Ru(bpy)_3^{2+}$ data yielded an activation energy around 4200 cm^{-1}, while the $Os(bpy)_3^{2+}$ value was approximately 420 cm^{-1}, or about one tenth of the ruthenium value. The bpy-based compounds *cis*-$Ru(bpy)_2(X)_2$, where X is either NCS^- or CN^-, exhibited temperature-dependent activation to only one upper excited state with activation energies less than 1000 cm^{-1}. The fully deprotonated, tetraanionic $(TBA)_4[Ru(dcb)_2(NCS)_2]$ compound exhibited thermal population to two different upper excited states with one activation energy less than 1000 cm^{-1} and the other around 4600 cm^{-1} as described above.

The sensitizer *cis*-$Ru(dcbH_2)_2(NCS)_2$ was attached to base pretreated TiO_2 and ZrO_2, *cis*-$Ru(dcb)_2(NCS)_2/TiO_2$, and *cis*-$Ru(dcb)_2(NCS)_2/ZrO_2$. Under these conditions, steady-state PL was observed upon light excitation of the sensitized thin films. The PL spectrum measured for $Ru(dcb)_2(NCS)_2/ZrO_2$ was in line with that expected for this sensitizer and was slightly broader than that observed in fluid solution. The *cis*-$Ru(dcb)_2(NCS)_2/TiO_2$ PL spectrum was red-shifted by 720 cm^{-1} relative to *cis*-$Ru(dcb)_2(NCS)_2/ZrO_2$. The spectrum was also broadened in comparison with the solution data. Pulsed light excitation of *cis*-$Ru(dcb)_2(NCS)_2/TiO_2$ led to a short-lived PL decay that was adequately described by a first-order kinetic model; see Figure 4A. Temperature-dependent lifetimes were analyzed from −40.0 to +40.0 °C with an activation energy of 690 cm^{-1} abstracted from the data as shown in Figure 4A. The PL decays of *cis*-$Ru(dcb)_2(NCS)_2/ZrO_2$ obtained from −40.0 to +70.0 °C could not be adequately described by a first-order kinetic model and fit well to a biexponential model. The fast and slow kinetic components of the PL decays were analyzed using a global fit to the activation energy with independent k_0 and k_1 terms for each component yielding an activation energy of 890 cm^{-1}; see Figure 4B. The excited-state decay parameters from the Arrhenius analyses for *cis*-$Ru(dcb)_2(NCS)_2/TiO_2$ and *cis*-$Ru(dcb)_2(NCS)_2/ZrO_2$ are collected in Table 3. The PL decay kinetics were found to be independent of the observation wavelength for both *cis*-$Ru(dcb)_2(NCS)_2/TiO_2$ and *cis*-$Ru(dcb)_2(NCS)_2/ZrO_2$.

Photolysis of $(TBA)_4[Ru(dcb)_2(NCS)_2]$ with 510 nm light was performed in acetonitrile at +70 °C for 3 h. After

dx.doi.org/10.1021/ic302339a | *Inorg. Chem.* 2013, 52, 6839−6848

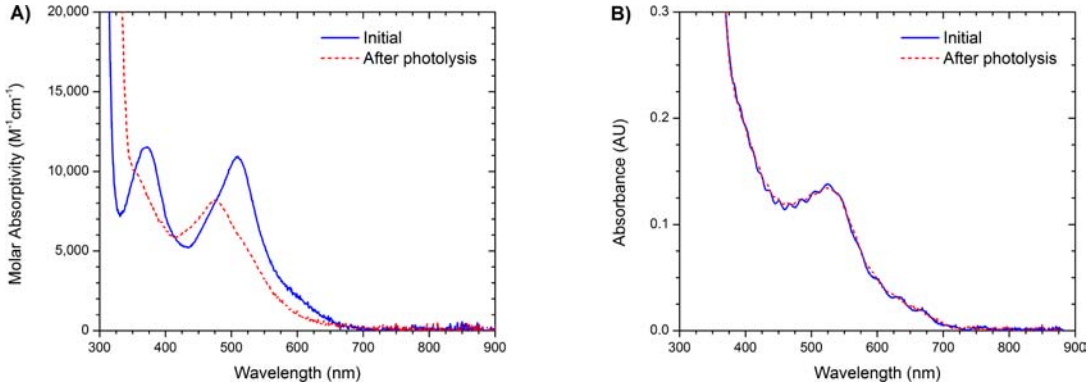

Figure 5. Absorption spectra of (A) $(TBA)_4[Ru(dcb)_2(NCS)_2]$ and (B) $Ru(dcb)_2(NCS)_2/TiO_2$ in CH_3CN before and after photolysis at +70 °C for 3 h.

photolysis, the lowest energy MLCT maximum blue-shifted from 507 to 475 nm and decreased in intensity, Figure 5A. Photolysis of $Ru(dcb)_2(NCS)_2/TiO_2$ with 532 nm excitation under otherwise identical conditions did not lead to any significant change in the UV−vis absorbance spectrum, Figure 5B.

DISCUSSION

The activated relaxation pathways abstracted from temperature-dependent measurements for $[cis\text{-}Ru(dcb)_2(NCS)_2]^{4-*}$ and $cis\text{-}Ru(dcb)_2(NCS)_2{}^*/TiO_2$ are summarized in Scheme 3. The

Scheme 3

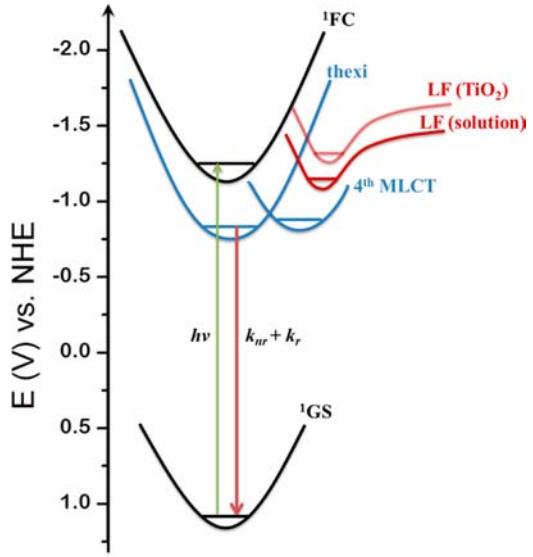

potential energy surfaces for the ground, thexi, and Franck−Condon (^{1}FC) states were placed on the indicated electrochemical scale from previously reported data.[32] We emphasize that our data provide the activation energy between states, not necessarily their absolute values. Therefore, the minima for the fourth MLCT and the LF states are unknown. The analysis implies that the activation energy for internal conversion from the thexi state to ligand field (LF) states increased when the compound was anchored to the semiconductor surface. Furthermore, under all conditions studied, the LF states were not as accessible to these MLCT excited states as the spectrochemical series would predict. Below we discuss the kinetic modeling from which the activational parameters were abstracted, followed by a discussion of the photophysical behavior in fluid solution and at metal oxide interfaces.

Kinetic Modeling. The detailed studies of Crosby and co-workers mentioned in the Introduction were performed for $Ru(bpy)_3{}^{2+}$ immobilized in polymethylmethacrylate (PMMA) thin films from 4 to 350 K.[1,2] Quantum yield and lifetimes data enabled the temperature dependence of both the radiative and the nonradiative rate constants to be quantified. Measurements below 5 K were required to resolve the three closely spaced electronic states that have significant Boltzmann population and behave as one state near room temperature. Since this pioneering work, there have been no subsequent studies of this scope. Far more common is to measure excited-state lifetimes over a limited temperature range as is reported herein.[4,5,64−68] With temperatures above the fluid-to-glass transition of the solvent, the data are often described by a single activational process plus a constant, k_0, eq 3.

$$\frac{1}{\tau_{obs}} = k_0 + A_1 \exp\left(\frac{-E_a}{k_B T}\right) \quad (3)$$

Some researchers have elected to fix k_0 to a limiting value measured at lower temperatures.[4,65] In these studies, this procedure was problematic as the lifetimes were temperature dependent over all ranges studied and fixing k_0 to discrete values led to quantitatively different activational parameters. The k_0 value was therefore allowed to float in the minimization process. Equation 3 was found to satisfactorily fit all of the data described herein with only one exception in $(TBA)_4[Ru(dcb)_2(NCS)_2]^*$ where a second activational process was needed. We note that the activational energy reported herein differs from that reported previously by Balzani and co-workers for $cis\text{-}Ru(bpy)_2(CN)_2$; their experimental data were in good agreement with our own, but the kinetic analysis differed.[31]

Fluid Solution. The activational parameters abstracted from excited-state relaxation of $Ru(bpy)_3{}^{2+*}$ and $Os(bpy)_3{}^{2+*}$ were in good agreement with previously published data.[4,67] Internal conversion from the thexi state to ligand field states, $(t_{2g})^5(\pi^*)^1 \rightarrow (t_{2g})^5(e_g{}^*)^1$, was irreversible with pre-exponential factors of 10^{14} s^{-1} and E_a of 4200 cm^{-1}. For $Os(bpy)_3{}^{2+*}$, the temperature range afforded by the acetonitrile or propylene carbonate solvents did not enable significant population of the ligand field states. Instead, a small temperature dependence was observed from which pre-exponential factors of 10^8 s^{-1} and E_a of 420 cm^{-1} were abstracted, parameters that are consistent with relaxation through the fourth MLCT excited state.[4,67]

dx.doi.org/10.1021/ic302339a | Inorg. Chem. 2013, 52, 6839−6848

Excited-state relaxation of *cis*-$Ru(bpy)_2X_2$ can, in principle, be predicted on the basis of the data for $Ru(bpy)_3^{2+}$* and the spectrochemical series.[69] Replacement of one bpy ligand with two strong field CN^- ligands would be expected to raise the energy of the LF states and, assuming similar force constants, increase the activation energy. Indeed, at the highest temperatures utilized (+100 °C in propylene carbonate), there was no experimental evidence for thexi → LF internal conversion for *cis*-$Ru(bpy)_2(CN)_2$*, and excited-state relaxation was very similar to that measured for $Os(bpy)_3^{2+}$* with contributions from only the fourth MLCT excited state.

Isothiocyanate is a weak field ligand positioned above the halides on the opposite end of the spectrochemical series with respect to cyanide.[69] Therefore, one would expect the ligand field states to be readily accessible from the MLCT excited state of *cis*-$Ru(bpy)_2(NCS)_2$. Surprisingly, this was not found to be the case, and excited-state relaxation occurred through the fourth MLCT excited state. In fact, based on the spectrochemical series, it is surprising in the first place that *cis*-$Ru(bpy)_2(NCS)_2$* displays room temperature photoluminescence with a lifetime of ~30 ns because related compounds with stronger field pyridine ligands, that is, *cis*-$Ru(bpy)_2(py)_2^{2+}$*, are nonemissive at room temperature with short excited-state lifetimes and high quantum yields for photochemical ligand loss, behavior consistent with facile population of antibonding ligand field states.[29,30,70−72] In the vast literature of isothiocyanate coordination chemistry as an ambidentate ligand, NCS^- is always considered a σ-donor with no π-accepting behavior.[73,74] Some more recent data, however, suggest that this is not necessarily the case.[75−79]

Schugar and co-workers noted that *cis*-$Ru(bpy)_2(NCS)_2$ displayed only a single ν_{CN} stretch.[60] Similar behavior was recently reported for a series of compounds of the type *cis*-$Ru(LL)_2(NCS)_2$.[76] The appearance of one single absorption band was surprising in two regards. First, a single IR absorption band was more consistent with the *trans*-form of the compound and the presence of an inversion center even though the geometry of these compounds and those in the present study clearly was *cis*-. Second, both an antisymmetric and symmetric ν_{CN} stretches were expected, yet only the single band was observed. This has been rationalized on the basis of the importance of two different resonance structures shown in Scheme 4.[75,76] Backbonding into the π* orbitals of resonance

Scheme 4

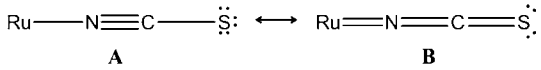

structure A is approximately equivalent to backbonding to bipyridine, which diminishes the energy separation between the antisymmetric and symmetric ν_{CN} combinations. X-ray crystallographic data were analyzed to check for evidence of π backbonding of this nature in the solid state.[60,77−79] The five crystal structures of *cis*-$Ru(LL)_2(NCS)_2$ compounds exhibit an average N−C bond length of 1.13 Å that is consistent with an N−C triple bond and inconsistent with π backbonding from the Ru center. However, the average C−S bond length from crystal data is 1.65 Å that is intermediate between a C−S single bond, 1.81 Å, and a C−S double bond, 1.55 Å.[69] Therefore, the crystallographic data provide some support for the proposal that π backbonding into the nitrile portion of resonance structure A in Scheme 4 is operative in the ground state.

The above discussion suggests that $NCS^- \rightarrow Ru^{II}$ backbonding may be more important in these compounds than the spectrochemical series predicts, at least in the ground electronic state. The ligand field strength in the excited state is potentially a more complicated issue. Upon light excitation, an electron is transferred from the Ru d-orbitals to the π* levels of the bpy ligand, eq 4.

$$cis\text{-}Ru^{II}(bpy)_2(NCS)_2 + h\nu \rightarrow cis\text{-}Ru^{III}(bpy^-)(bpy)(NCS)_2^* \quad (4)$$

The ligand field splitting parameter Δ_o is expected to be 30% larger for Ru^{III} than for Ru^{II}.[69,80] However, the formal oxidation states are most relevant to the initial formed Franck−Condon excited state because intersystem crossing and vibrational relaxation transfer charge back to the metal center in the thexi state. Nevertheless, the excited state is more Ru^{III} like than is the ground state. The appearance of absorption bands in the near-infrared region for both the excited and the oxidized state has been previously assigned as ligand-to-metal charge transfer absorptions and provides direct evidence for $NCS^- \rightarrow$ Ru. Theoretical studies also indicated partial "hole transfer" from the Ru to the sulfur atom in the isothiocyanate ligand.[81−84] Furthermore, electrochemical measurements have shown that the isothiocyanate oxidation is proximate to the metal centered $Ru^{III/II}$ redox process.[85,86]

The coordinated isothiocyanate ligand can be viewed as two resonance forms, Scheme 4. Kaim has shown that upon oxidation of *cis*-$Ru^{II}(LL)_2(NCS)_2$, the decreased electron density at the ruthenium center promotes a structural conversion from A to B.[76] Indeed, recent time-resolved X-ray data indicate that the Ru−N(NCS) bond length decreases by 0.06 Å upon oxidation.[87] This may represent the most significant inner-sphere reorganization in these compounds that display unusually small reorganization energies for MLCT excitation[88] and excited-state electron transfer.[35]

The inductive effect brought about by substitution of the bipyridine ligands in the 4,4′-positions can rationalize the temperature dependence of *cis*-$Ru(bpy)_2(NCS)_2$, *cis*-$Ru(dcbH_2)_2(NCS)_2$, and $(TBA)_4[Ru(dcb)_2(NCS)_2]$. The electron-withdrawing carboxylic acid groups stabilize the thexi state, thereby increasing the thexi−LF energy gap. On the other hand, carboxylate acts as an electron donor, such that $(TBA)_4[Ru(dcb)_2(NCS)_2]$ has the smallest thexi−LF energy gap. It is for this reason that the LF state population was only observed for this excited state.

Metal Oxide Interfaces. Steady-state photoluminescence was observed from *cis*-$Ru(dcbH_2)_2(NCS)_2$ anchored to mesoporous thin films of insulating ZrO_2 and semiconducting TiO_2, abbreviated $Ru(dcb)_2(NCS)_2/MO_2$. The PL from $Ru(dcb)_2(NCS)_2/TiO_2$ was enhanced by a pretreatment of the TiO_2 thin films with aqueous base.[44−46] This treatment shifts the acceptor states in TiO_2 negative on an electrochemical scale (i.e., toward the vacuum level). Previous studies on closely related sensitized materials have shown that this pretreatment lowers the excited-state injection yield measured when the films are immersed in neat acetonitrile.[89,90] Indeed under such conditions, the TiO_2 behaves more like an insulator in that the MLCT excited state does not undergo efficient electron transfer and the photophysical behavior was very similar to that observed for $Ru(dcb)_2(NCS)_2/ZrO_2$.

Lateral intermolecular energy transfer is known to complicate kinetic analysis of MLCT excited-state relaxation on semi-

dx.doi.org/10.1021/ic302339a | Inorg. Chem. 2013, 52, 6839−6848

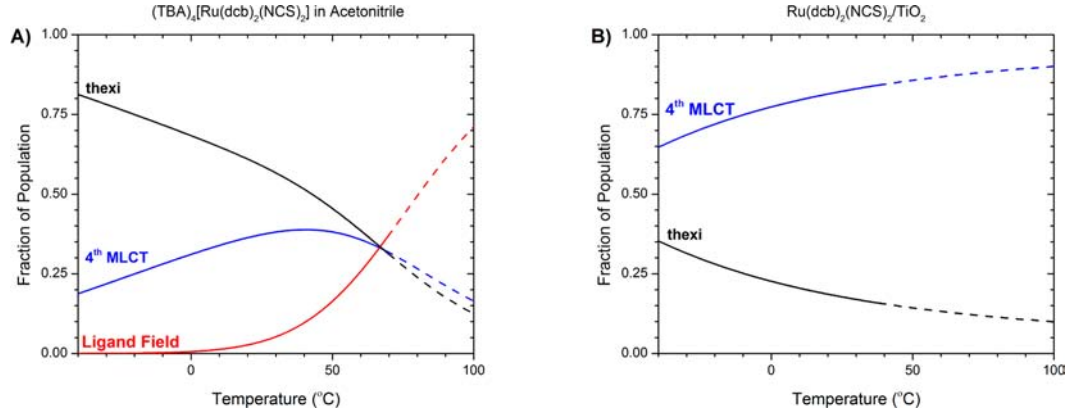

Figure 6. The fraction of excited states that relax through the thexi (black), fourth MLCT (blue), and LF (red) states as a function of temperature for (A) *cis*-$Ru(dcb)_2(NCS)_2^{4-}$ in CH_3CN and (B) $Ru(dcb)_2(NCS)_2/TiO_2$ thin film immersed in CH_3CN. The dashed lines are predictions based on the experimental data from lower temperatures shown as solid lines.

conductor surfaces.[49−51] Energy migration leads to triplet−triplet annihilation reactions that are second-order in excited-state concentration. Monte−Carlo simulations were consistent with a $(30\ ns)^{-1}$ energy hopping rate for $Ru(bpy)_3^{2+}$ type sensitizers.[49] In the present work, excited-state decay was satisfactorily described by a first-order kinetic model, presumably because the irradiance was kept low and the short excited-state lifetimes resulted in inefficient energy transfer.

Infrared measurements were consistent with previous studies that indicate all of the carboxylic acid groups are deprotonated in the $Ru(dcb)_2(NCS)_2/MO_2$ thin films.[91,92] The fully deprotonated compound, $(TBA)_4[Ru(dcb)_2(NCS)_2]$, is therefore a better model for the surface behavior than is *cis*-$Ru(dcbH_2)_2(NCS)_2$. The key difference in excited-state relaxation observed in solution relative to the metal oxide surfaces was that there was no evidence for ligand field population at the oxide interfaces. Presumably, relaxation through the ligand field states had a much larger barrier for the metal oxide surface than it did in fluid solution. Indeed, previous studies have shown that entrapment of $Ru(bpy)_3^{2+}$ in zeolites and polymers also resulted in an increased activation energy for LF state population.[24,25,29,30,72,93] Population of the LF states results in an elongation of metal−ligand bonds that is restricted by the metal oxide surface. As a result, the excited states are expected to be more stable toward photochemical ligand loss when anchored to a TiO_2 nanocrystallite.

In this regard, it is of interest to compare excited-state relaxation pathways of $(TBA)_4[Ru(dcb)_2(NCS)_2]$ with $Ru(dcb)_2(NCS)_2/TiO_2$ in acetonitrile solution. The fraction of excited states that decay through each pathway are shown as a function of temperature in Figure 6.[4,67] In fluid solution at +67 °C, excited-state relaxation occurs with equal probability through the thexi, fourth MLCT, and LF states. In contrast, at the same temperature, 13% decay through the thexi state with 87% through the fourth MLCT state for $Ru(dcb)_2(NCS)_2/TiO_2$.

Consistent with this model, steady-state photolysis at the MLCT maximum showed very different behavior for the sensitizer in fluid solution and anchored to TiO_2 thin films at +70 °C. Photolysis of *cis*-$Ru(dcb)_2(NCS)_2^{4-}$ in CH_3CN at +70 °C led to spectral changes consistent with ligand loss photochemistry. In contrast, excitation of $Ru(dcb)_2(NCS)_2/TiO_2$ under the same conditions of temperature and solvent gave no evidence for photochemistry.

CONCLUSION

The temperature-dependent lifetime data of *cis*-$Ru(bpy)_2(CN)_2$ and *cis*-$Ru(bpy)_2(NCS)_2$ were well described by an Arrhenius model from which activation energies of 810 cm^{-1} and pre-exponential factors of $\sim 10^8\ s^{-1}$ were abstracted. By analogy to previously reported data for MLCT excited states, these activational parameters were attributed to population of a higher lying "fourth" MLCT excited state. Notably absent was the expected population of antibonding ligand field states for *cis*-$Ru(bpy)_2(NCS)_2$, behavior that was attributed to π−bonding into the NCS^- ligand and partial charge transfer from the NCS^- to the metal center in the excited state. The inductive influence of substituents in the 4 and 4′ positions of the bpy ligands was also quantified. The introduction of electron-withdrawing carboxylic acid groups in *cis*-$Ru(dcbH_2)_2(NCS)_2$ increased the energy gap between the thexi and LF states. Carboxylate groups in *cis*-$Ru(dcb)_2(NCS)_2^{4-}$ resulted in excited states that relaxed through the fourth MLCT and LF states. Excited-state relaxation of the compound anchored to TiO_2, $Ru(dcb)_2(NCS)_2/TiO_2$, was through the thexi and fourth MLCT states without evidence for thexi → LF state internal conversion. Therefore, the temperature-dependent lifetime data predicted that $Ru(dcb)_2(NCS)_2/TiO_2$ would be stable with regard to ligand loss photochemistry, a prediction that was supported by photolysis experiments at +70 °C. This finding is also consistent with previous studies that attributed ligand loss photochemistry of $Ru(dcb)_2(NCS)_2/TiO_2$ to the oxidized form of the compound,[94−96] which has long been known to be reactive.[97]

AUTHOR INFORMATION

Corresponding Author

*E-mail: meyer@jhu.edu.

Notes

The authors declare no competing financial interest.

ACKNOWLEDGMENTS

This research is based upon work supported by the National Science Foundation and a Graduate Research Fellowship under Grant No. DGE-1232825.

REFERENCES

(1) Hager, G. D.; Crosby, G. A. *J. Am. Chem. Soc.* **1975**, *97*, 7031−7037.
(2) Hager, G. D.; Watts, R. J.; Crosby, G. A. *J. Am. Chem. Soc.* **1975**, *97*, 7037−7042.
(3) Crosby, G. A.; Demas, J. N. *J. Am. Chem. Soc.* **1971**, *93*, 2841−2847.
(4) Lumpkin, R. S.; Kober, E. M.; Worl, L. A.; Murtaza, Z.; Meyer, T. J. *J. Phys. Chem.* **1990**, *94*, 239−243.
(5) Sykora, M.; Kincaid, J. R. *Inorg. Chem.* **1995**, *34*, 5852−5856.
(6) Alary, F.; Heully, J. L.; Bijeire, L.; Vicendo, P. *Inorg. Chem.* **2007**, *46*, 3154−3165.
(7) Harriman, A.; Izzet, G. *Phys. Chem. Chem. Phys.* **2007**, *9*, 944−948.
(8) Demas, J. N.; Taylor, D. G. *Inorg. Chem.* **1979**, *18*, 3177−3179.
(9) Demas, J. N.; Crosby, G. A. *J. Mol. Spectrosc.* **1968**, *26*, 72−77.
(10) Crosby, G. A.; Hipps, K. W.; Elfring, W. H. *J. Am. Chem. Soc.* **1974**, *96*, 629−630.
(11) Fan, J.; Tysoe, S.; Strekas, T. C.; Gafney, H. D.; Serpone, N.; Lawless, D. *J. Am. Chem. Soc.* **1994**, *116*, 5343−5351.
(12) Pinnick, D. V.; Durham, B. *Inorg. Chem.* **1984**, *23*, 1440−1445.
(13) Pinnick, D. V.; Durham, B. *Inorg. Chem.* **1984**, *23*, 3841−3842.
(14) Wright, D. W.; Schmehl, R. H. *Inorg. Chem.* **1990**, *29*, 155−157.
(15) Wacholtz, W. M.; Auerbach, R. A.; Schmehl, R. H.; Ollino, M.; Cherry, W. R. *Inorg. Chem.* **1985**, *24*, 1758−1760.
(16) Reveco, P.; Schmehl, R. H.; Cherry, W. R.; Fronczek, F. R.; Selbin, J. *Inorg. Chem.* **1985**, *24*, 4078−4082.
(17) Henderson, L. J.; Cherry, W. R. *Chem. Phys. Lett.* **1985**, *114*, 553−556.
(18) Chaisson, D. A.; Hintze, R. E.; Stuermer, D. H.; Petersen, J. D.; McDonald, D. P.; Ford, P. C. *J. Am. Chem. Soc.* **1972**, *94*, 6665−6673.
(19) Malouf, G.; Ford, P. C. *J. Am. Chem. Soc.* **1977**, *99*, 7213−7221.
(20) Carlos, R. M.; Neumann, M. G.; Tfouni, E. *Inorg. Chem.* **1996**, *35*, 2229−2234.
(21) Singh, T. N.; Turro, C. *Inorg. Chem.* **2004**, *43*, 7260−7262.
(22) Allsopp, S. R.; Cox, A.; Kemp, T. J.; Reed, W. J. *J. Chem. Soc., Faraday Trans.* **1978**, *74*, 1275−1289.
(23) Masschelein, A.; Mesmaeker, A. K.-D.; Willsher, C. J.; Wilkinson, F. *J. Chem. Soc., Faraday Trans.* **1991**, *87*, 259−267.
(24) Maruszewski, K.; Strommen, D. P.; Kincaid, J. R. *J. Am. Chem. Soc.* **1993**, *115*, 8345−8350.
(25) Maruszewski, K.; Kincaid, J. R. *Inorg. Chem.* **1995**, *34*, 2002−2006.
(26) Kitamura, N.; Sato, M.; Kim, H.-B.; Obata, R.; Tazuke, S. *Inorg. Chem.* **1988**, *27*, 651−658.
(27) Kober, E. M.; Sullivan, B. P.; Meyer, T. J. *Inorg. Chem.* **1984**, *23*, 2098−2104.
(28) Chen, P.; Meyer, T. J. *Chem. Rev.* **1998**, *98*, 1439−1478.
(29) Thompson, D. W.; Fleming, C. N.; Myron, B. D.; Meyer, T. J. *J. Phys. Chem. B* **2007**, *111*, 6930−6941.
(30) Calvert, J. M.; Meyer, T. J. *Inorg. Chem.* **1982**, *21*, 3978−3989.
(31) Barigelletti, F.; Juris, A.; Balzani, V.; Belser, P.; Von Zelewsky, A. *J. Phys. Chem.* **1987**, *91*, 1095−1098.
(32) Nazeeruddin, M. K.; Kay, A.; Rodicio, I.; Humphry-Baker, R.; Mueller, E.; Liska, P.; Vlachopoulos, N.; Grätzel, M. *J. Am. Chem. Soc.* **1993**, *115*, 6382−6390.
(33) Ardo, S.; Meyer, G. J. *Chem. Soc. Rev.* **2009**, *38*, 115−164.
(34) Grätzel, M. *Acc. Chem. Res.* **2009**, *42*, 1788−1798.
(35) Grätzel, M. *Inorg. Chem.* **2005**, *44*, 6841−6851.
(36) Hannappel, T.; Burfeindt, B.; Storck, W.; Willig, F. *J. Phys. Chem. B* **1997**, *101*, 6799−6802.
(37) Kallioinen, J.; Benkö, G.; Myllyperkiö, P.; Khriachtchev, L.; Skårman, B.; Wallenberg, R.; Tuomikoski, M.; Korppi-Tommola, J.; Sundström, V.; Yartsev, A. P. *J. Phys. Chem. B* **2004**, *108*, 6365−6373.
(38) Benkö, G.; Kallioinen, J.; Myllyperkiö, P.; Trif, F.; Korppi-Tommola, J. E. I.; Yartsev, A. P.; Sundström, V. *J. Phys. Chem. B* **2004**, *108*, 2862−2867.
(39) Benkö, G.; Kallioinen, J.; Korppi-Tommola, J. E. I.; Yartsev, A. P.; Sundström, V. *J. Am. Chem. Soc.* **2001**, *124*, 489−493.
(40) Kuciauskas, D.; Monat, J. E.; Villahermosa, R.; Gray, H. B.; Lewis, N. S.; McCusker, J. K. *J. Phys. Chem. B* **2002**, *106*, 9347−9358.
(41) Smeigh, A. L.; Katz, J. E.; Brunschwig, B. S.; Lewis, N. S.; McCusker, J. K. *J. Phys. Chem. C* **2008**, *112*, 12065−12068.
(42) Listorti, A.; O'Regan, B.; Durrant, J. R. *Chem. Mater.* **2011**, *23*, 3381−3399.
(43) Asbury, J. B.; Anderson, N. A.; Hao, E.; Ai, X.; Lian, T. *J. Phys. Chem. B* **2003**, *107*, 7376−7386.
(44) Enright, B.; Redmond, G.; Fitzmaurice, D. *J. Phys. Chem.* **1994**, *98*, 6195−6200.
(45) Lyon, L. A.; Hupp, J. T. *J. Phys. Chem. B* **1999**, *103*, 4623−4628.
(46) Clark, W. D. K.; Sutin, N. *J. Am. Chem. Soc.* **1977**, *99*, 4676−4682.
(47) Qu, P.; Thompson, D. W.; Meyer, G. J. *Langmuir* **2000**, *16*, 4662−4671.
(48) Farzad, F.; Thompson, D. W.; Kelly, C. A.; Meyer, G. J. *J. Am. Chem. Soc.* **1999**, *121*, 5577−5578.
(49) Higgins, G. T.; Bergeron, B. V.; Hasselmann, G. M.; Farzad, F.; Meyer, G. J. *J. Phys. Chem. B* **2006**, *110*, 2598−2605.
(50) Ardo, S.; Meyer, G. J. *J. Am. Chem. Soc.* **2011**, *133*, 15384−15396.
(51) Kelly, C. A.; Farzad, F.; Thompson, D. W.; Meyer, G. J. *Langmuir* **1999**, *15*, 731−737.
(52) Koops, S. E.; Durrant, J. R. *Inorg. Chim. Acta* **2008**, *361*, 663−670.
(53) Heimer, T. A.; Meyer, G. J. *J. Lumin.* **1996**, *70*, 468−478.
(54) Vinodgopal, K.; Hua, X.; Dahlgren, R. L.; Lappin, A. G.; Patterson, L. K.; Kamat, P. V. *J. Phys. Chem.* **1995**, *99*, 10883−10889.
(55) Fessenden, R. W.; Kamat, P. V. *J. Phys. Chem.* **1995**, *99*, 12902−12906.
(56) Nazeeruddin, M. K.; Zakeeruddin, S. M.; Humphry-Baker, R.; Jirousek, M.; Liska, P.; Vlachopoulos, N.; Shklover, V.; Fischer, C.-H.; Grätzel, M. *Inorg. Chem.* **1999**, *38*, 6298−6305.
(57) Heimer, T. A.; D'Arcangelis, S. T.; Farzad, F.; Stipkala, J. M.; Meyer, G. J. *Inorg. Chem.* **1996**, *35*, 5319−5324.
(58) Crosby, G. A.; Demas, J. N. *J. Phys. Chem.* **1971**, *75*, 991−1024.
(59) Kober, E. M.; Caspar, J. V.; Lumpkin, R. S.; Meyer, T. J. *J. Phys. Chem.* **1986**, *90*, 3722−3734.
(60) Herber, R. H.; Nan, G.; Potenza, J. A.; Schugar, H. J.; Bino, A. *Inorg. Chem.* **1989**, *28*, 938−942.
(61) Wajda, S.; Rachlewicz, K. *Inorg. Chim. Acta* **1978**, *31*, 35−40.
(62) Kohle, O.; Ruile, S.; Grätzel, M. *Inorg. Chem.* **1996**, *35*, 4779−4787.
(63) Zakeeruddin, S. M.; Nazeeruddin, M. K.; Humphry-Baker, R.; Grätzel, M. *Inorg. Chim. Acta* **1999**, *296*, 250−253.
(64) Wacholtz, W. F.; Auerbach, R. A.; Schmehl, R. H. *Inorg. Chem.* **1986**, *25*, 227−234.
(65) Abrahamsson, M.; Becker, H.-C.; Hammarström, L.; Bonnefous, C.; Chamchoumis, C.; Thummel, R. P. *Inorg. Chem.* **2007**, *46*, 10354−10364.
(66) Abrahamsson, M.; Wolpher, H.; Johansson, O.; Larsson, J.; Kritikos, M.; Eriksson, L.; Norrby, P.-O.; Bergquist, J.; Sun, L.; Åkermark, B.; Hammarström, L. *Inorg. Chem.* **2005**, *44*, 3215−3225.
(67) Forster, L. S. *Coord. Chem. Rev.* **2002**, *227*, 59−92.
(68) Cherry, W. R.; Henderson, L. J. *Inorg. Chem.* **1984**, *23*, 983−986.
(69) Miessler, G. L.; Tarr, D. A. *Inorganic Chemistry*, 4th ed.; Prentice Hall: Upper Saddle River, NJ, 2011.
(70) Durham, B.; Walsh, J. L.; Carter, C. L.; Meyer, T. J. *Inorg. Chem.* **1980**, *19*, 860−865.
(71) Rillema, D. P.; Blanton, C. B.; Shaver, R. J.; Jackman, D. C.; Boldaji, M.; Bundy, S.; Worl, L. A.; Meyer, T. J. *Inorg. Chem.* **1992**, *31*, 1600−1606.
(72) Adelt, M.; Devenney, M.; Meyer, T. J.; Thompson, D. W.; Treadway, J. A. *Inorg. Chem.* **1998**, *37*, 2616−2617.
(73) Burmeister, J. *Coord. Chem. Rev.* **1990**, *105*, 77−133.
(74) Norbury, A. H. *J. Chem. Soc. A* **1971**, 1089−1091.
(75) Asbury, J. B.; Ellingson, R. J.; Ghosh, H. N.; Ferrere, S.; Nozik, A. J.; Lian, T. *J. Phys. Chem. B* **1999**, *103*, 3110−3119.

(76) Kämper, S.; Paretzki, A.; Fiedler, J.; Záliš, S.; Kaim, W. *Inorg. Chem.* **2012**, *51*, 2097−2104.
(77) Shklover, V.; Nazeeruddin, M. K.; Zakeeruddin, S. M.; Barbé, C.; Kay, A.; Haibach, T.; Steurer, W.; Hermann, R.; Nissen, H. U.; Grätzel, M. *Chem. Mater.* **1997**, *9*, 430−439.
(78) Shklover, V.; Ovchinnikov, Y. E.; Braginsky, L. S.; Zakeeruddin, S. M.; Grätzel, M. *Chem. Mater.* **1998**, *10*, 2533−2541.
(79) Tuikka, M.; Hirva, P.; Rissanen, K.; Korppi-Tommola, J.; Haukka, M. *Chem. Commun.* **2011**, *47*, 4499−4501.
(80) Meyer, T. J. *Pure Appl. Chem.* **1986**, *58*, 1193.
(81) Guillemoles, J.-F.; Barone, V.; Joubert, L.; Adamo, C. *J. Phys. Chem. A* **2002**, *106*, 11354−11360.
(82) Nazeeruddin, M. K.; De Angelis, F.; Fantacci, S.; Selloni, A.; Viscardi, G.; Liska, P.; Ito, S.; Takeru, B.; Grätzel, M. *J. Am. Chem. Soc.* **2005**, *127*, 16835−16847.
(83) Rensmo, H.; Södergren, S.; Patthey, L.; Westermark, K.; Vayssieres, L.; Kohle, O.; Brühwiler, P. A.; Hagfeldt, A.; Siegbahn, H. *Chem. Phys. Lett.* **1997**, *274*, 51−57.
(84) Fantacci, S.; De Angelis, F. *Coord. Chem. Rev.* **2011**, *255*, 2704−2726.
(85) Wolfbauer, G.; Bond, A. M.; Deacon, G. B.; MacFarlane, D. R.; Spiccia, L. *J. Am. Chem. Soc.* **1999**, *122*, 130−142.
(86) Bond, A. M.; Deacon, G. B.; Howitt, J.; MacFarlane, D. R.; Spiccia, L.; Wolfbauer, G. *J. Electrochem. Soc.* **1999**, *146*, 648−656.
(87) Zhang, X.; Smolentsev, G.; Guo, J.; Attenkofer, K.; Kurtz, C.; Jennings, G.; Lockard, J. V.; Stickrath, A. B.; Chen, L. X. *J. Phys. Chem. Lett.* **2011**, *2*, 628−632.
(88) Shoute, L. C. T.; Loppnow, G. R. *J. Am. Chem. Soc.* **2003**, *125*, 15636−15646.
(89) Kelly, C. A.; Farzad, F.; Thompson, D. W.; Stipkala, J. M.; Meyer, G. J. *Langmuir* **1999**, *15*, 7047−7054.
(90) Qu, P.; Meyer, G. J. *Langmuir* **2001**, *17*, 6720−6728.
(91) Finnie, K. S.; Bartlett, J. R.; Woolfrey, J. L. *Langmuir* **1998**, *14*, 2744−2749.
(92) Nazeeruddin, M. K.; Humphry-Baker, R.; Liska, P.; Grätzel, M. *J. Phys. Chem. B* **2003**, *107*, 8981−8987.
(93) Vaidyalingam, A.; Dutta, P. K. *Anal. Chem.* **2000**, *72*, 5219−5224.
(94) Nour-Mohhamadi, F.; Nguyen, S. D.; Boschloo, G.; Hagfeldt, A.; Lund, T. *J. Phys. Chem. B* **2005**, *109*, 22413−22419.
(95) Nguyen, H. T.; Ta, H. M.; Lund, T. *Sol. Energy Mater. Sol. Cells* **2007**, *91*, 1934−1942.
(96) Andersen, A. R.; Halme, J.; Lund, T.; Asghar, M. I.; Nguyen, P. T.; Miettunen, K.; Kemppainen, E.; Albrektsen, O. *J. Phys. Chem. C* **2011**, *115*, 15598−15606.
(97) Das, S.; Kamat, P. V. *J. Phys. Chem. B* **1998**, *102*, 8954−8957.